



**HAL**  
open science

## Force Control System for an Automotive Semi-active Suspension

Carlos A Vivas-Lopez, Diana A Hernández-Alcántara, Manh Quan Nguyen,  
Ruben Morales-Menendez, Olivier Sename

► **To cite this version:**

Carlos A Vivas-Lopez, Diana A Hernández-Alcántara, Manh Quan Nguyen, Ruben Morales-Menendez, Olivier Sename. Force Control System for an Automotive Semi-active Suspension. LPVS 2015 - 1st IFAC Workshop on Linear Parameter Varying Systems, Oct 2015, Grenoble, France. hal-01412892

**HAL Id: hal-01412892**

**<https://hal.science/hal-01412892>**

Submitted on 9 Dec 2016

**HAL** is a multi-disciplinary open access archive for the deposit and dissemination of scientific research documents, whether they are published or not. The documents may come from teaching and research institutions in France or abroad, or from public or private research centers.

L'archive ouverte pluridisciplinaire **HAL**, est destinée au dépôt et à la diffusion de documents scientifiques de niveau recherche, publiés ou non, émanant des établissements d'enseignement et de recherche français ou étrangers, des laboratoires publics ou privés.

## Force Control System for an Automotive Semi-active Suspension <sup>\*</sup>

Carlos A. Vivas-Lopez <sup>\*</sup> Diana Hernández-Alcántara <sup>\*</sup>  
Manh-Quan Nguyen <sup>\*\*</sup> Ruben Morales-Menendez <sup>\*</sup>  
Olivier Sename <sup>\*\*</sup>

<sup>\*</sup> *Tecnológico de Monterrey, School of Engineering and Sciences  
Av. E. Garza Sada 2501, Monterrey, NL, México  
{A00794204, A00469139, rmm}@itesm.mx*

<sup>\*\*</sup> *CNRS-Grenoble INP, GIPSA-lab, 11 rue des Mathématiques 38402  
St Martin d'Hères cedex, France  
{manh-quan.nguyen, olivier.sename}@gipsa-lab.grenoble-inp.fr*

**Abstract:** A new semi-active suspension control system is proposed. This control system includes a *Linear Parameter Varying (LPV)* controller which was designed to improve the ride comfort. It also incorporates a *Force Control System (FCS)* to transform the force command from the *LPV* controller to a input signal for the *Electro-Rheological (ER)* semi-active damper. This *FCS* was assessed by its tracking performance of the desired force command, with a 7 % of tracking error. Then the semi-active control system was evaluated in a *Quarter of Vehicle (QoV)* model under two tests: a *Bump* and a *Road Profile*. The results were a reduction up to 19 % (*Bump* test) and 29 % (*Road Profile* test), of the sprung mass position compared with a passive suspension. Additionally, an improvement up to 14 % was obtained when compared with a *LPV* controller using a simple model inversion *Force-Manipulation* transformation.

*Keywords:* LPV systems, Automotive semi-active dampers, Electro-Rheological shock absorber

### 1. INTRODUCTION

The way a suspension system is tuned in the vehicle design process can affect ride comfort and road holding. Therefore, a passive suspension has to be designed to achieve a good compromise between these goals.

To overcome these passive damper limitations, semi-active shock absorbers can be used. These type of devices can on-line change their dissipation characteristics. Technologies such as *Electro-Rheological (ER)* or *Magneto-Rheological (MR)* are the most commercially used because of their advantages: fast time response (40 ms), large force range, wide bandwidth of control and cost.

*ER* damper force dynamic is highly non-linear (i.e. saturation, hysteresis, etc.). Figure 1 presents the *Force-Velocity (FV)* map of an *ER* shock absorber. These effects can be well modelled by equations that mimic the damper force ( $F_D$ ) as a function of the damper deflection ( $z_{def}$ ), deflection velocity ( $\dot{z}_{def}$ ), and manipulation signal ( $v$ ), Guo et al. (2006):

$$F_D = c_p(\dot{z}_{def}) + k_p(z_{def}) + F_{sa} \quad (1)$$

where  $F_{sa} = v \cdot f_c \cdot \tanh(a_1(\dot{z}_{def}) + a_2(z_{def}))$  is the semi-active force due to  $v$ . Table 1 resumes the description of the variables.

Semi-active suspensions require a control system to maintain a desired performance. Normally, those controllers are

<sup>\*</sup> Authors thank CONACyT and CRNS for their partial support in the bilateral México-France PCP projects 03/10 and 06/13.

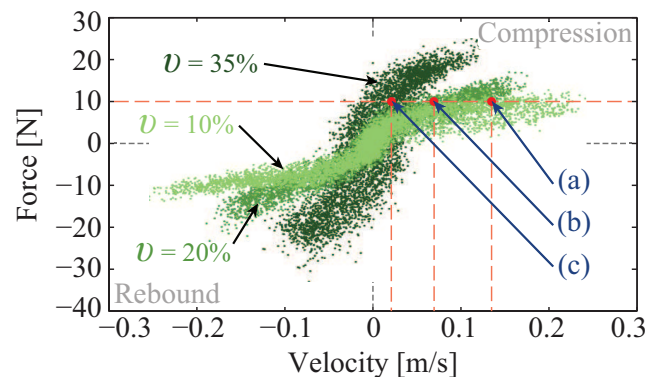


Fig. 1. Force-velocity map for different duty cycles.

designed to calculate a force that meets that performance, but a transformation from force to manipulation ( $v$ ) is needed. Because of the non-linear damper characteristics, it is possible to achieve the same level of force at different conditions. As an example, the three red points in Fig. 1 (a, b, and c) correspond to the same  $F_D = 10$  N but, all are achieved at different *average* velocities and manipulations; (a) 0.12 m/s with 10 %, (b) 0.08 m/s with 20 %, and (c) 0.02 m/s with 35 %. Moreover, the actuator dynamics cannot be neglected, Priyandoko et al. (2009). This condition makes the mapping from force to manipulation not a trivial task hence a tracking control system is needed.

This problem has been addressed in previous works. Kitching et al. (1998) used a cascade control system, the master controller tracks the desired damper force, whereas the

slave one controls the opening valve position of the flow. Only the damper velocity was considered to compute the control algorithm and the damper force loop had a considerable delay. A neural network of the inverse model of the damper force was proposed in Chang and Zhou (2002). The desired force and two steps of the damper displacement are needed to obtain the manipulation. Hudha et al. (2005) used a *PI* controller coupled with *conditional* rules, however they do not take into account the dynamic of the damper force during the *PI* tuning. Similarly, Sam and Hudha (2006) proposed a *PI* controller and incorporated the dynamics of the damper flow valve; but the considered actuator was active thus did not consider the dissipativity restrictions of the semi-active dampers. Finally, Pellegrini et al. (2011) proposed an inverse model of the damper to obtain the manipulation, but they neglected the dynamic of the damper.

Unlike previous authors, this work proposes a *Force Control System (FCS)* that overcomes the non-linear force constraints of the damper by considering its dynamical response. This *FCS* is designed to operate along with a *Linear Parameter Varying (LPV)* controller for a semi-active suspension control system.

This paper is organized as follows. Section 2 describes the automotive semi-active suspension and its control system. Section 3 shows the design of the proposed *FCS*. Section 4 discusses the results. Finally, section 5 concludes the paper.

Table 1. Description of variables.

Variable	Description	Units
$z_r$	Road profile	m
$z_s, z_{us}$	Sprung/Unsprung mass position	m
$z_{def}, z_{def_t}$	Damper/Tire deflection	m
$\dot{z}_s, \dot{z}_{us}, \dot{z}_{def}$	Sprung/Unsprung mass velocity, damper deflection velocity	m/s
$\ddot{z}_s, \ddot{z}_{us}$	Sprung/Unsprung mass acceleration	m/s <sup>2</sup>
$F_D$	Damper Force	N
$c_p$	Viscous damping coefficient	N·s/m
$k_p$	Stiffness coefficient	N/m
$F_{sa}$	Semi-active component of the damper force	N
$v$	% of Manipulation	%
$a_1$	Hysteresis coefficient due to velocity	N·s/m
$a_2$	Hysteresis coefficient due to displacement	N/m
$f_c$	Damping coefficient	N/%
$k_s, k_t$	Spring/Tire stiffness	N/m
$m_s, m_{us}$	Sprung/Unsprung mass	kg
$\omega_d$	Natural frequency	rad
$k_d$	Static gain	
$m_d$	Dynamic damping coefficient	

## 2. AUTOMOTIVE SUSPENSION SYSTEM

Figure 2 presents the block diagram of the *LPV* control system. This control system is designed using the *Quarter of Vehicle (QoV)* model.

### 2.1 QoV Model

The *QoV* model is used to analyse the vertical dynamics of a vehicle. It represents a quarter of the vehicle body with the wheel, tire, and suspension elements (spring and damper) with the following equations:

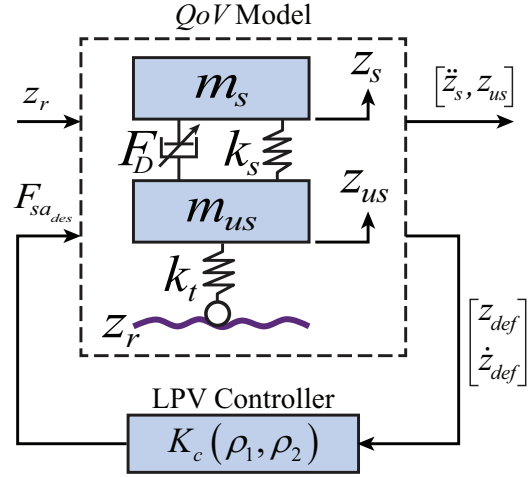


Fig. 2. *LPV* control system.

$$\begin{aligned} m_s \ddot{z}_s &= -F_D - k_s(z_s - z_{us}) \\ m_{us} \ddot{z}_{us} &= k_s(z_s - z_{us}) + F_D - k_t(z_{us} - z_r) \end{aligned} \quad (2)$$

where  $F_D$  is computed with two equations: 1) a static model and 2) a dynamical model, Fig. 3.

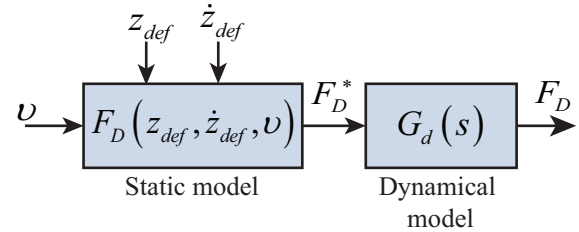


Fig. 3. Damper model.

The static force of the damper is calculated using (1). The dynamical behaviour is represented as a second order system, Aubouet (2010):

$$G_d(s) = \frac{F_D(s)}{F_D^*(s)} = \frac{k_d}{(1/\omega_d^2)s^2 + (2m_d/\omega_d)s + 1} \quad (3)$$

### 2.2 LPV Semi-Active Suspension Controller

A *Linear Parameter Varying (LPV)* controller is used. This controller incorporates in its design the characteristics of saturation and hysteresis of the semi-active damper to fulfill its force constraints, Do et al. (2010).

Substituting (1) in (2), and using  $f_v = v \cdot f_c$ :

$$\begin{aligned} m_s \ddot{z}_s &= -k_s(z_s - z_{us}) - c_p(\dot{z}_s - \dot{z}_{us}) - k_p(z_s - z_{us}) \\ &\quad - f_v \tanh(a_1(\dot{z}_{def}) + a_2(z_{def})) \\ m_{us} \ddot{z}_{us} &= k_s(z_s - z_{us}) + c_p(\dot{z}_s - \dot{z}_{us}) + k_p(z_s - z_{us}) \\ &\quad + f_v \tanh(a_1(\dot{z}_{def}) + a_2(z_{def})) - k_t(z_{def_t}) \end{aligned} \quad (4)$$

To satisfy the dissipativity constraint of a semi-active damper,  $f_v$  must be constrained by

$$0 < f_{v_{min}} \leq f_v \leq f_{v_{max}} \quad (5)$$

defining  $u_v = f_v - F_0$ , with  $F_0 = (f_{v_{min}} + f_{v_{max}})/2$ , the dissipativity constraint on  $f_v$  is recast as a saturation constraint on  $u_v$ , i.e.

$$-F_I \leq u_v \leq F_I \quad (6)$$

where  $F_I = (f_{v_{max}} - f_{v_{min}})/2$ .

Denoting  $k_f = k_s + k_p$ ,  $z_{def} = z_s - z_{us}$ ,  $z_{def_i} = z_{us} - z_r$ , and  $\hat{\rho} = \tanh(a_1(\dot{z}_s - \dot{z}_{us}) + a_2(z_s - z_{us}))$ , a state space representation of (4) is:

$$P: \begin{cases} \dot{x}_s = A_s x_s + B_s \hat{\rho} f_v + B_{sw} w \\ z = C_{sz} x_s + D_{sz} \hat{\rho} f_v \\ y = C_s x_s \end{cases} \quad (7)$$

where  $x_s = (z_s, \dot{z}_s, z_{us}, \dot{z}_{us})^T$ ,  $w = z_r$ ,  $y = (z_{def}, \dot{z}_{def})^T$ .

$$A_s = \begin{pmatrix} 0 & 1 & 0 & 0 \\ -\frac{k_f}{m_s} & -\frac{c_p}{m_s} & \frac{k_f}{m_s} & \frac{c_p}{m_s} \\ 0 & 0 & 0 & 1 \\ \frac{k_f}{m_{us}} & \frac{c_p}{m_{us}} & -\frac{k_f + k_t}{m_{us}} & -\frac{c_p}{m_{us}} \end{pmatrix}, B_s = \begin{pmatrix} 0 \\ 1 \\ 0 \\ 1 \\ m_{us} \end{pmatrix}$$

$$B_{sw} = \begin{pmatrix} 0 \\ 0 \\ 0 \\ k_t \\ m_{us} \end{pmatrix}, C_s = \begin{pmatrix} 1 & 0 & -1 & 0 \\ 0 & 1 & 0 & -1 \end{pmatrix}^T$$

$$C_{sz} = \begin{pmatrix} -\frac{k_f}{m_s} & -\frac{c_p}{m_s} & \frac{k_f}{m_s} & \frac{c_p}{m_s} \\ 0 & 0 & 1 & 0 \end{pmatrix}, D_{sz} = \begin{pmatrix} -1 \\ m_s \\ 0 \end{pmatrix}$$

The control input of (7) is parameter-dependent and it can be rewritten as follows:

$$\begin{cases} \dot{x} = A(\rho_1, \rho_2) x + B u + B_1 w \\ z = C_z(\rho_1, \rho_2) x \\ y = C x \end{cases} \quad (8)$$

where:

$$x = \begin{pmatrix} x_s \\ x_f \end{pmatrix}, A(\rho_1, \rho_2) = \begin{pmatrix} A_s + \rho_2 B_{s1} C_{s1} & \rho_1 B_s C_f \\ 0 & A_f \end{pmatrix},$$

$$B = \begin{pmatrix} 0 \\ B_f \end{pmatrix}, B_1 = \begin{pmatrix} B_{sw} \\ 0 \end{pmatrix}, C = \begin{pmatrix} C_s \\ 0 \end{pmatrix}^T,$$

$$C_z(\rho_1, \rho_2) = (C_{sz} + \rho_2 D_{s1} C_{s1} \quad \rho_1 D_{sz} C_f)$$

$$B_{s1} = \begin{pmatrix} 0 & -\frac{F_0}{m_s} & 0 & \frac{F_0}{m_{us}} \end{pmatrix}^T, C_{s1} = (a_2 \quad a_1 \quad -a_2 \quad -a_1),$$

$$D_{s1} = \begin{pmatrix} -F_0 & 0 \\ m_s & 0 \end{pmatrix}$$

$$\rho_1 = \tanh(C_{s1} x_s) \tanh\left(\frac{C_f x_f}{F_1}\right) \frac{F_1}{C_f x_f}, \rho_2 = \frac{\tanh(C_{s1} x_s)}{C_{s1} x_s}$$

$x_f, A_f, B_f, C_f$  are the matrices corresponding to a state space representation of the low-pass filter  $W_{filter} = w_f/(s + w_f)$  which is added to the system to make the control input matrices parameter-independent.

The LPV controller, scheduled by  $\rho_1, \rho_2$ , has the form:

$$K_c(\rho_1, \rho_2): \begin{cases} \dot{x}_c = A_c(\rho_1, \rho_2) x_c + B_c(\rho_1, \rho_2) y \\ u^{H_\infty} = C_c(\rho_1, \rho_2) x_c \end{cases} \quad (9)$$

This controller minimizes the  $H_\infty$ -norm of the transfer function between the input disturbances  $w$  and controlled outputs  $z$ . The synthesis of the controller is made in the LPV/ $H_\infty$  framework based on the LMI solution, see Scherer et al. (1997), for polytopic systems with quadratic stabilization, Do et al. (2010).

### 3. FORCE CONTROL SYSTEM

The LPV controller output ( $F_{sa_{des}}$ ) cannot go directly to the semi-active damper as an input, it needs to be transformed into a manipulation signal ( $v$ ). This signal is considered as a percentage of the possible range manipulation input. This transformation becomes complicated because of the non-linear behaviour of the damper, Fig. 1.

In addition to the LPV controller output ( $F_{sa_{des}}$ ),  $z_{def}$  and  $\dot{z}_{def}$  are needed to obtain the corresponding  $v$ . In addition, the dynamics of the damper must be considered. Hence, a simple inverse model is not enough, then a FCS is proposed. The FCS has two objectives: 1) to bound  $F_{sa_{des}}$  in a possible force range ( $F_{sa_{des}}^*$ ) and 2) to compute the required  $v$  input to achieve the desired damper force. Figure 4 shows the proposed semi-active suspension control system; the FCS is shown in detail.

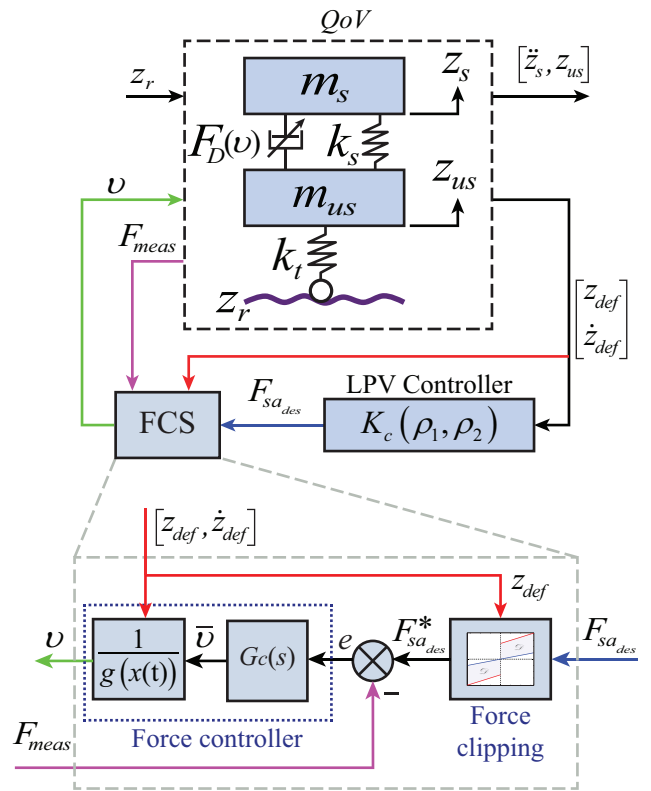


Fig. 4. LPV semi-active control system including the FCS.

#### 3.1 Control System Design

The FCS takes as reference the LPV output ( $F_{sa_{des}}$ ) and sends the corresponding manipulation ( $v$ ) to the damper, Fig. 4. In the first place it is necessary to ensure that  $F_{sa_{des}}$  can be delivered by the ER damper. This is done by defining an admissible region ( $\mathcal{D}$ ) which includes the achievable force range of the real damper, Poussot-Vassal et al. (2008). To bound the force a clipping function is used:

$$\mathcal{D}(F_D, \dot{z}_{def}) \mapsto F_D^* = \begin{cases} F_D & \text{if } F_D \in \mathcal{D} \\ F_D^\perp & \text{if } F_D \notin \mathcal{D} \end{cases} \quad (10)$$

where an orthogonal projection of the desired force ( $F_D^\perp$ ) over the region  $\mathcal{D}$  is assumed, this projection is driven

by the current measure of the damper velocity. Figure 5 presents the admissible region  $\mathcal{D}$  and the simulated force for different percentages of manipulation.

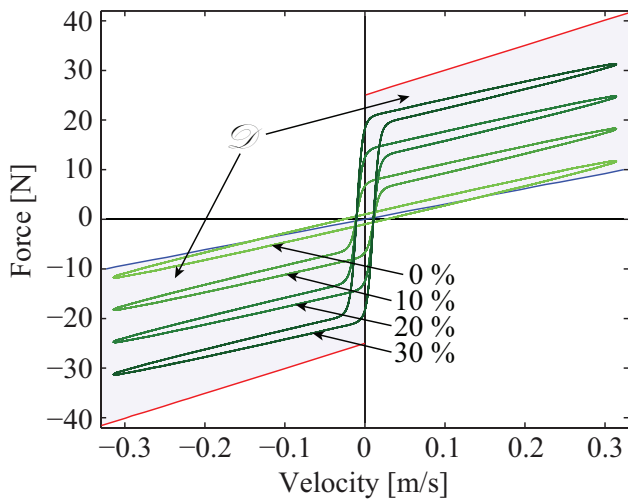


Fig. 5. Admissible force region ( $\mathcal{D}$ ) and damper force at different manipulation levels.

Considering the *ER* damper model, the following control law is proposed:

$$v = g(x(t))^{-1} \bar{v} \quad (11)$$

with

$$G_c(s) = \frac{\bar{v}(s)}{e(s)} \quad (12)$$

where  $g(x(t)) = f_c \cdot \tanh(a_1 \dot{z}_{def} + a_2 z_{def})$  and  $e(t) = F_{sa_{des}}(t) - F_{sa}(t)$ .

The controller  $G_c(s)$ , (12), is designed using the dynamic model (3), and classical control techniques, considering the following specifications: bandwidth around 100 rad/s, gain and phase margin greater than 12 dB and 45° respectively. A controller which fulfil these specifications is given by:

$$G_c(s) = \frac{86(s + 120)}{s(s + 80)} \quad (13)$$

#### 4. RESULTS

The evaluation of the semi-active suspension control system is made in two steps: 1) Assessment of the *FCS* using the tracking error of the force as the performance index, and 2) evaluation of the control system at different tests, this evaluation is held in time and frequency domains.

##### 4.1 Force Control System Assessment

To evaluate the performance of the *FCS*, a reference of force ( $F_{sa_{des}}$ ) that mimics the characteristics and behaviour of an automotive semi-active damper under normal operating conditions is needed. For this purpose an *ER* shock absorber was simulated under different displacements ( $z_{def}$ ), velocities ( $\dot{z}_{def}$ ) and manipulations ( $v$ ) inputs to generate a force reference ( $F_{sa_{des}}$ ). The selected signals are summarized in Table 2.

Figure 6 shows the response of the *FCS*. The *Root-Mean-Square (RMS)* value of the tracking error is used as

Table 2. Design of Experiments for the *FCS*. Displacement of 5 mm.

Test	Displacement		Manipulation	
	Signal	$f$ [Hz]	Signal	Characteristics
1	Sin	1	Square	$f = 2$ Hz, $A \in [10, 30]$ %
2	Chirp	[1-10]		
3	Triangular	1		

performance index. Table 3 presents the *RMS* index of the tracking error and its normalization against the force range ( $F_{D_{max}} - F_{D_{min}}$ ) corresponding to each test.

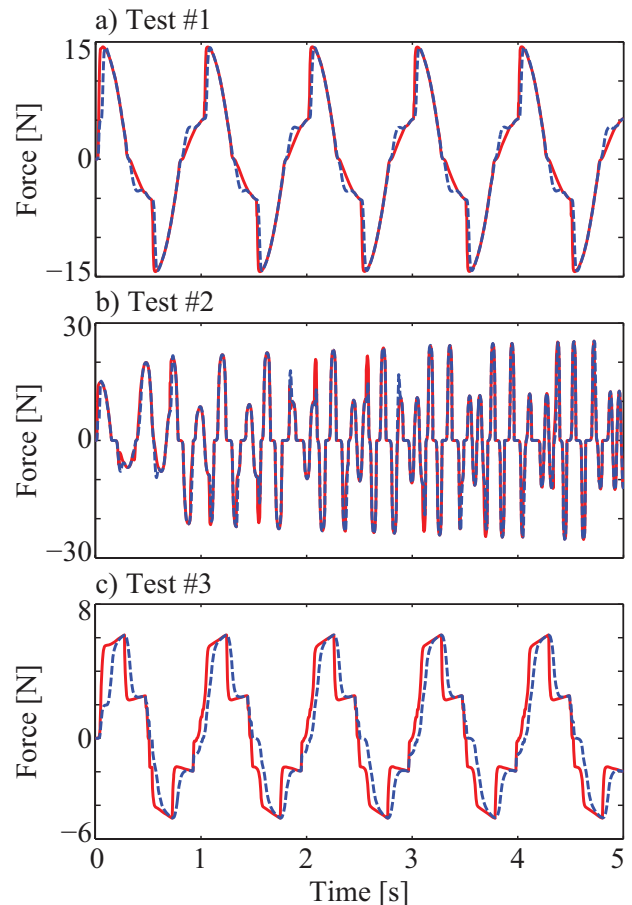


Fig. 6. Comparison of reference force (solid red) and the achieved force (dashed blue) at different displacement inputs to the damper model.

A qualitative analysis can be made based on Fig. 6. It can be seen that the proposed *FCS* was able to follow the reference signal, even for the *Chirp* signal, where the frequency of the wave increased up to 10 Hz.

Table 3. Tracking error of different tests.

Test	#1	#2	#3
<i>RMS</i>	1.63	2.01	1.42
Normalized <i>RMS</i>	5.66 %	3.96 %	13.14 %

A quantitative analysis was made by using Table 3. The *RMS* errors from the different experiments show that the *FCS* was able to track the reference for the different signals. In the test # 2 with the *Chirp* signal, the error is higher, but not considerably. The error in Test # 3 is considerably high, but in this case the force reference

behaves as a square signal (i.e. the worst case). It can be concluded that the controller is able to follow the reference signal and the tracking error can be neglected.

4.2 Semi-active Suspension Control System Evaluation

To evaluate the performance of the proposed control system, three cases were compared: 1) A passive suspension system where the ER damper manipulation was fixed at 20 % (*Passive*), 2) the proposed control system (*LPV + FCS*) and 3) a *LPV* controller coupled with a *Simple Model Inversion (LPV + SMI)* function. The comparison was based on: ride comfort index, and road-holding index. In the *LPV + SMI* control system, the  $F_{sa_{des}}$  command was transformed from force to manipulation by using the next simple inverse model function:

$$v(F_{sa_{des}}) = \begin{cases} 35\% & \text{if } F_{sa_{des}} \geq f_c \cdot 35\% \\ F_{sa_{des}}\% & \text{if } f_c \cdot 10\% < F_{sa_{des}} < f_c \cdot 35\% \\ f_c & 10\% & \text{if } F_{sa_{des}} \leq f_c \cdot 10\% \end{cases} \quad (14)$$

this function substitutes the *FCS* block in Fig. 4.

*Time Domain Evaluation.* Figure 7 shows the results of a test with a *Bump* of 5 mm high, and Fig. 8 a test with a *Road Profile* input signal. Table 4 summarizes the *RMS* index. The reported indexes are computed as improvement of each variable against the *Passive* case, as:

$$\% \text{ of Improvement} = 1 - \frac{RMS(X_{iControlled})}{RMS(X_{iPassive})} \quad (15)$$

where  $X_i$  is the corresponding controlled variable ( $z_s$  or  $z_{def_t}$ ) for the control systems.

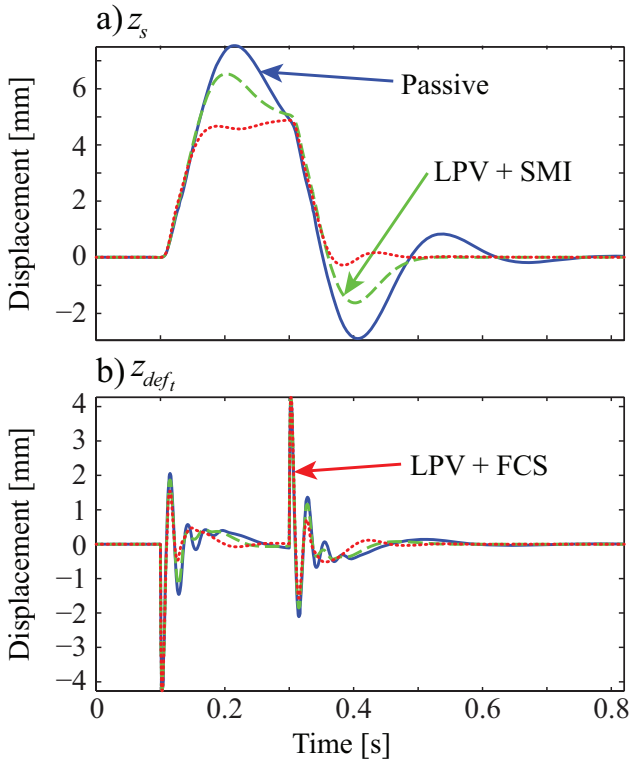


Fig. 7. Comparison of control systems for the Bump test.

Figure 7 shows the displacement of the sprung mass and the deflection of the tire for the *Bump* test. This test was used to evaluate the response of the system against a highly uncomfortable situation. Figure 7a shows that the *LPV + FCS* control system was able to compensate the effect of the *Bump* with a smooth transition, while the *Passive* case presents amplification of the *Bump* effect and oscillations in its transient response. For the *LPV + SMI* control system, the simplistic transformation of the force to manipulation introduces a negative impact in the performance. Figure 7b shows, in both cases an improvement on the tire deflection and in their transient behaviour, meaning less tire bounce. The *Passive* case presents higher oscillations in its transient response.

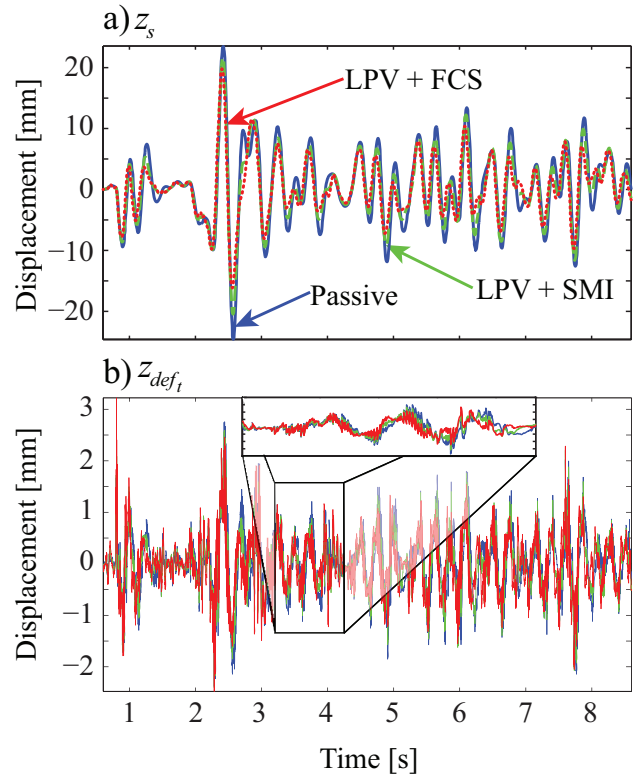


Fig. 8. Comparison of control systems for the Road Profile test.

Figure 8 compares the control systems for the *Road Profile* test. This test evaluates the performance of a control system in a common automotive operation condition during riding. Figure 8a shows how both control systems *LPV + SMI* and *LPV + FCS* reduce the movement of the sprung mass, having better performance the *LPV + FCS* case. Figure 8b shows the response of  $z_{def_t}$ ; it can be observed in the detail view that the *LPV + FCS* control system has a better performance.

Table 4 shows a quantitative comparison, it can be seen that the *LPV + FCS* controller has the better suspension performance. Regarding comfort, in the *Bump* test the improvement is considerably higher (19.14 %) compared with the *LPV + SMI* case (5.49 %), in both cases they were better than the *Passive* case. The same occurs in the *Road Profile* test where the *LPV + FCS* has a 29.38 % of improvement compared with the *Passive* case, against

Table 4. *RMS* index performance improvement.

Case	Variables	
	$z_s$	$z_{def_t}$
<b>Bump Test</b>		
<i>LPV + FCS</i>	19.14 %	12.09 %
<i>LPV + SMI</i>	5.49 %	5.31 %
<b>Road Profile Test</b>		
<i>LPV + FCS</i>	29.38 %	21.92 %
<i>LPV + SMI</i>	15.67 %	11.87 %

the 15.67 % obtained by the *LPV + SMI* control system. These results are consistent with the qualitative ones.

*Frequency Domain Evaluation.* Figure 9 presents the frequency response of  $z_s/z_r$ , and  $z_{def_t}/z_r$  functions, Poussot-Vassal et al. (2012). It can be seen that the *LPV + FCS* control system has better performance in comfort ( $z_s/z_r$ ) than both *Passive* and *LPV + SMI* cases, specially in the resonance frequencies. For the road-holding ( $z_{def_t}/z_r$ ) the *LPV + FCS* control system has also better performance in the range of 0-5 Hz. It can be seen that the use of the *FCS* improves the performance of the *LPV* control system.

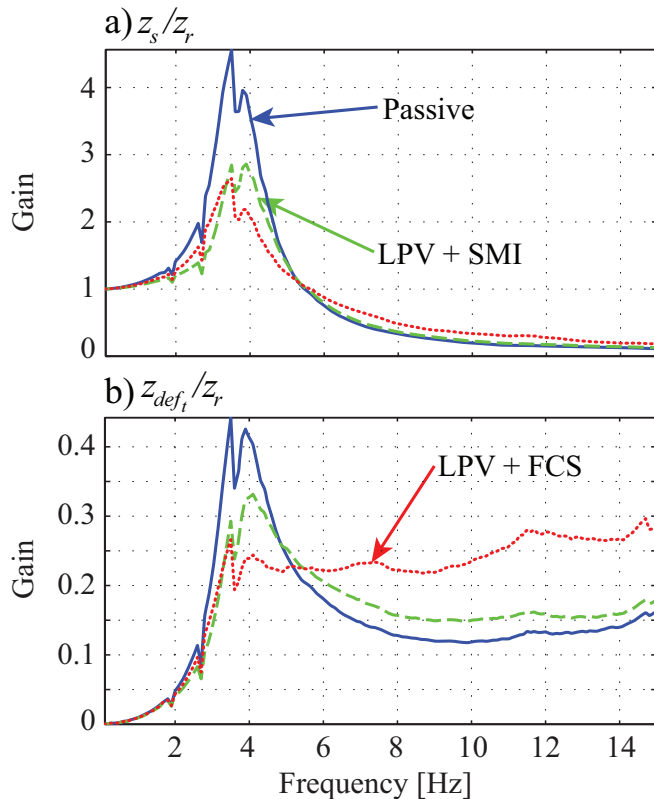


Fig. 9. Frequency responses of the variables of interest.

*Remark 1.* In the frequency analysis the range beyond 15 Hz was not take into account due to unmodeled dynamics in the mathematical model beyond that point.

## 5. CONCLUSIONS

A *Force Control System (FCS)* was proposed to improve a *Linear Parameter Varying (LPV)* control system. The *FCS* considers the non-linear dynamic behaviour of an *Electro-Rheological (ER)* damper, Fig. 1. Due to these

non-linearities, the damper can deliver wrong output manipulations in different conditions, the *FCS* adjusts the manipulation to reach the force reference, regardless the uncontrolled variables in the force control loop ( $z_{def}$ , and  $\dot{z}_{def}$ ).

In order to validate the proposal, the *LPV + FCS* control system was compared with a *LPV* plus a *Simple Model Inversion (SMI)* mapping function, taking the *Passive* case as reference. The *LPV + FCS* control system proved its effectiveness by maintaining the original control objectives with better performance in comfort and road-holding.

## REFERENCES

- Aubouet, S. (2010). *Semi-active SOBEN suspensions modeling and control*. Thesis, Institut National Polytechnique de Grenoble - INPG.
- Chang, C. and Zhou, L. (2002). Neural Network Emulation of Inverse Dynamics for a Magneto-Rheological Damper. *J. of Structural Eng.*, 128(2), 231–239.
- Do, A., Sename, O., and Dugard, L. (2010). An LPV Control Approach for Semi-Active Suspension Control with Actuator Constraints. In *American Control Conf.*, 4653–4658. USA.
- Guo, S., Yang, S., and Pan, C. (2006). Dynamical Modeling of Magneto-Rheological Damper Behaviors. *J. of Intell. Mater., Syst. and Struct.*, 17, 3–14.
- Hudha, K., Jamaluddin, H., Samin, P., and Rahman, R. (2005). Effects of Control Techniques and Damper Constraint on the Performance of a Semi-Active Magneto-Rheological Damper. *Int. J. Vehicle Autonomous Systems*, 3, 230–252.
- Kitching, K.J., Cole, D.J., and Cebon, D. (1998). Performance of a Semi-Active Damper for Heavy Vehicles. *J. Dyn. Sys., Meas., Control*, 122(3), 498–506.
- Pellegrini, E., Koch, G., Spirk, S., and Lohmann, B. (2011). A Dynamic Feedforward Control Approach for a Semi-Active Damper based on a New Hysteresis Model. In *18<sup>th</sup> IFAC World Congress*, 6248–6253. Italy.
- Poussot-Vassal, C., Sename, O., Dugard, L., Gáspár, P., Szabó, Z., and Bokor, J. (2008). A New Semi-Active Suspension Control Strategy through LPV Technique. *Control Eng. Practice*, 16, 1519–1534.
- Poussot-Vassal, C., Spelta, C., Sename, O., Savaresi, S., and Dugard, L. (2012). Survey and Performance Evaluation on Some Automotive Semi-Active Suspension Control Methods: A Comparative Study on a Single-Corner Model. *Annual Reviews in Control*, 36(1), 148–160.
- Priyandoko, G., Mailah, M., and Jamaluddin, H. (2009). Vehicle Active Suspension System using Sky-Hook Adaptive Neuro Active Force Control. *Mechanical Systems and Signal Processing*, 23, 855–68.
- Sam, Y. and Hudha, K. (2006). Modelling and Force Tracking Control of Hydraulic Actuator for an Active Suspension System. In *IEEE Conf. on Ind Electronics and Applications*, 1–6. Singapore.
- Scherer, C., Gahinet, P., and Chilali, M. (1997). Multiobjective Output-Feedback Control via LMI Optimization. *IEEE Trans on Automatic Control*, 42(7), 896–911.